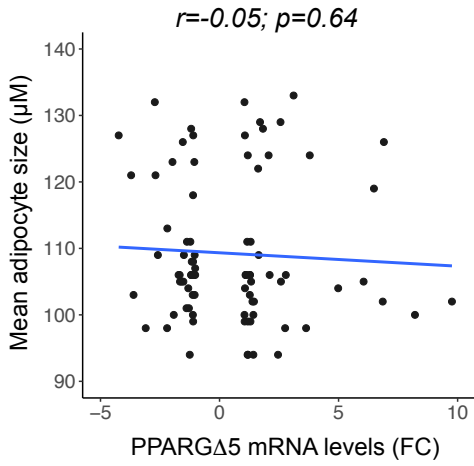
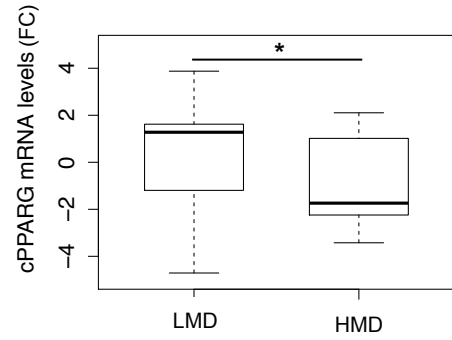


Figure S1

A



B



C

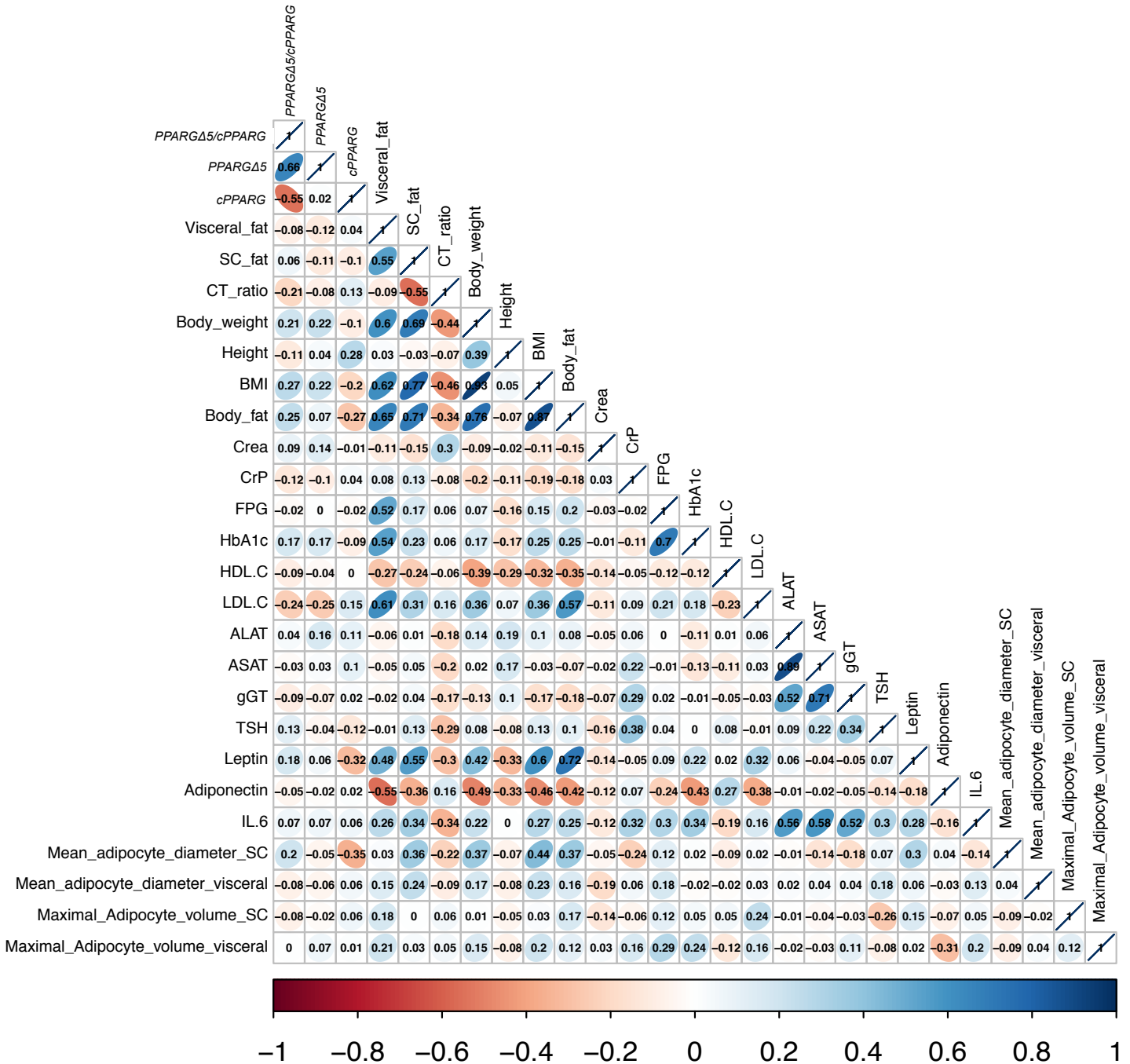


Figure S1. Correlation of PPARG Δ 5 and cPPARG levels with clinical and biochemical parameters

(A) Scatterplot resulting from regression analysis and showing correlation between PPARG Δ 5 levels and mean diameter of subcutaneous adipocyte size (N=86). Pearson correlation coefficient (r) and p value (p) are shown.

(B) Boxplot showing cPPARG levels in two subgroups, defined according to the mean diameter of subcutaneous adipocytes as “Low Mean Diameter” (LMD; mean diameter <115 μ m, N=63) and “High Mean Diameter” (HMD; mean diameter >115 μ m, N=23) group. *p<0.05.

(C) Corrplot reporting the Pearson’s correlation coefficients for cPPARG, PPARG Δ 5, PPARG Δ 5/cPPARG and several clinical and biochemical parameters. CT_ratio=VAT/SAT ratio by computed tomography, CREA=Creatinine, CRP=C-reactive protein, FPG=fasting plasma glucose, HbA1c=Hemoglobin A1c, HDL.C=High-Density Lipoprotein-Cholesterol, LDL.C=Low-Density Lipoprotein-Cholesterol, ALAT=Alanine aminotransferase, ASAT=Aspartate transaminase, gGT=gamma-glutamyl transpeptidase, SC=subcutaneous.

Figure S2

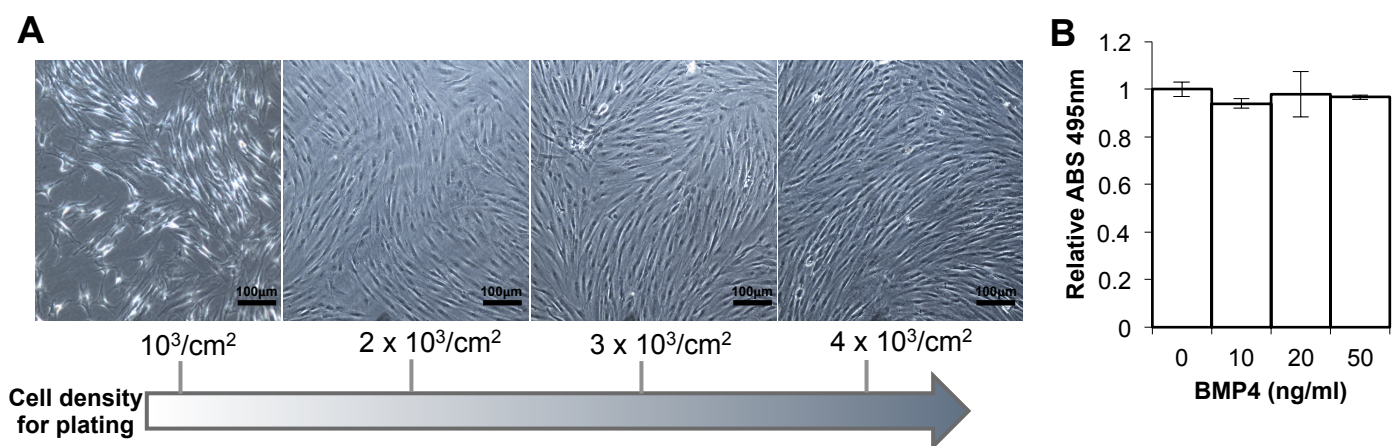


Figure S2. Adipocyte differentiation of hMSCs is affected by densities of cell plating

(A) Representative phase-contrast images of hMSCs plated at different densities (10^3 , 2×10^3 , 3×10^3 and $4 \times 10^3/\text{cm}^2$; scale bars, 100 μm).

(B) Lipid accumulation by oil Red O staining (optical density) of mature adipocytes differentiated from hMSCs with adipogenic mixes supplemented with increasing doses (i.e. 10, 20 and 50 ng/mL) of Bone Morphogenic Protein 4 (BMP4). Data are reported as mean \pm SEM vs cells treated with vehicle (0 ng/mL).

Figure S3

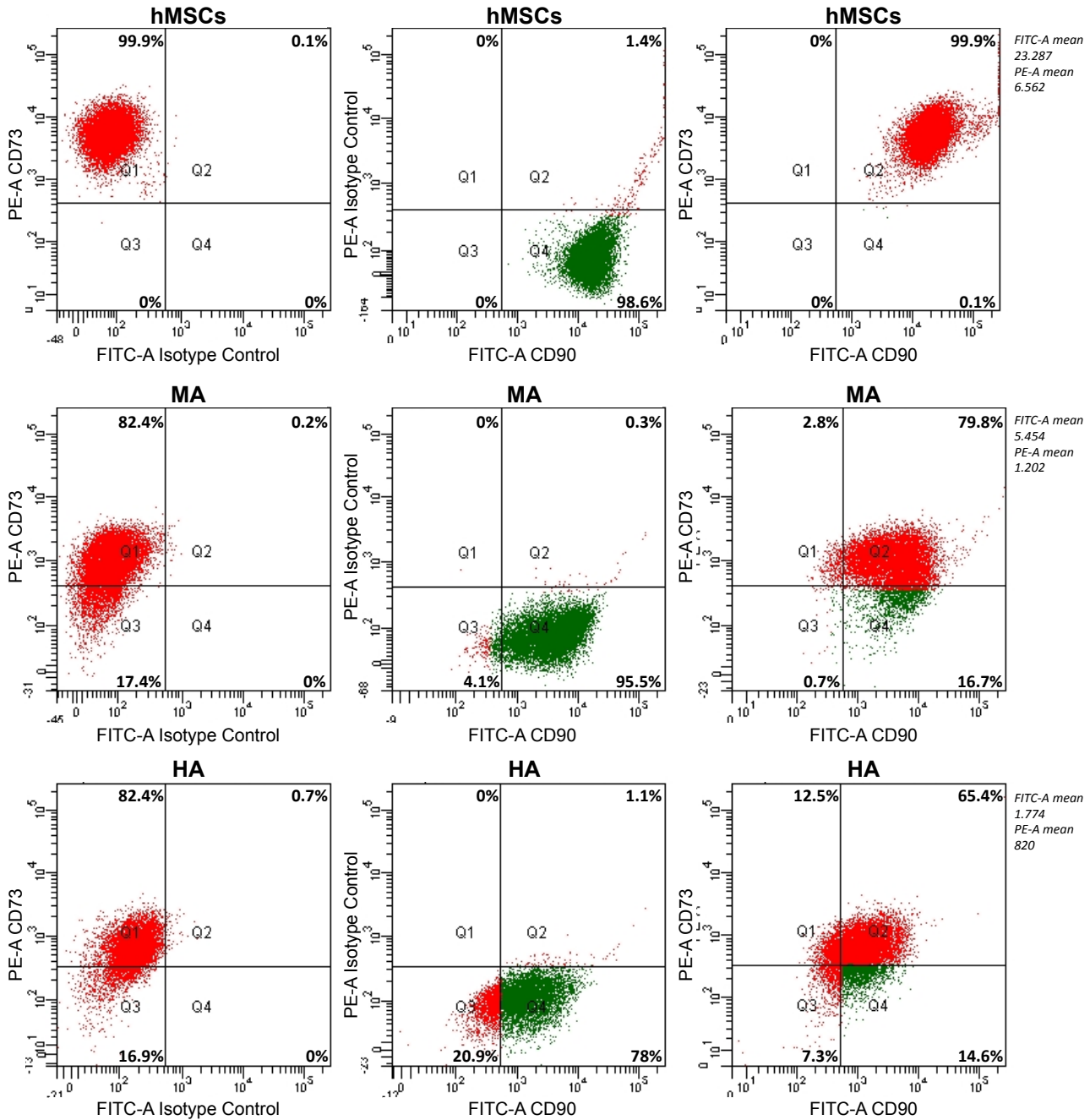


Figure S3. Stemness markers expression in terminally differentiated hMSCs and in hypertrophic-like cells

Flow cytometry analysis of CD73 and CD90 markers in hMSCs at starting point (hMSCs), in mature (MA) and hypertrophic-like adipocytes (HA). PE and FITC fluorophores were conjugated to anti-CD73 and anti-CD90 antibodies, respectively. Left boxes show expression values of FITC- and PE-isotype controls.

Figure S4

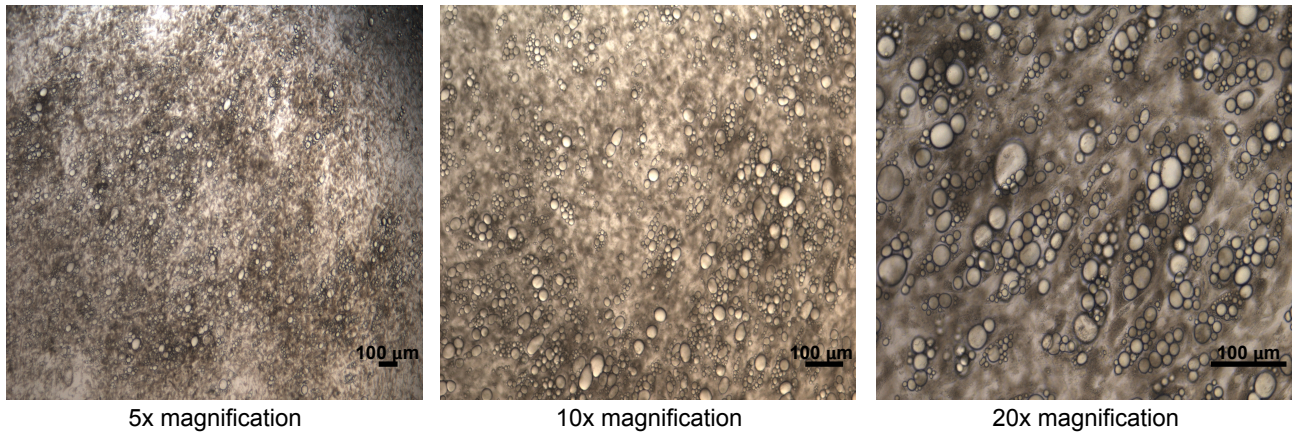


Figure S4. Hypertrophic-like adipocytes are less prone to dedifferentiation *in vitro*
Representative phase-contrast images at different magnifications cultured of hypertrophic-like adipocytes in standard conditions for additional 30 days (scale bars, 100 μm).

Figure S5

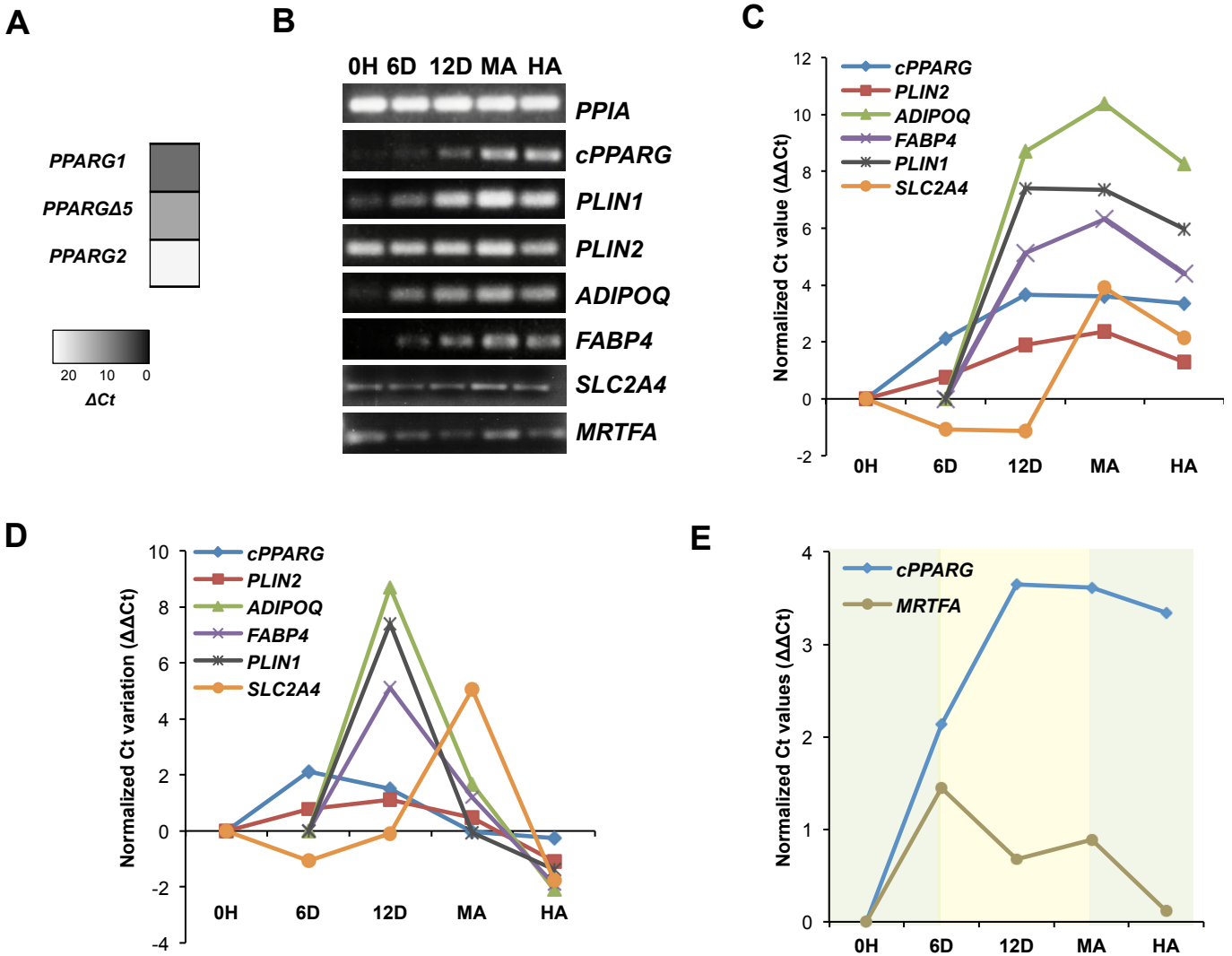


Figure S5. Expression trends of PPAR γ and its target genes

(A) Gray-scale heatmap of normalized mRNA expression values (i.e. $\Delta Ct = Ct \text{ gene} - Ct \text{ PPIA}$) of canonical (PPARG1 and PPARG2) and dominant negative (PPARG $\Delta 5$) PPARG transcripts determined by qPCR in hMSCs (T=0 hours). PPIA was used as reference gene.

(B) Representative gel images of RT-PCR assays in hMSCs at different time points upon adipogenic induction (T=0 hours, T=6 and T=12 days) and in mature and hypertrophic-like adipocytes (MAs and HAs, respectively).

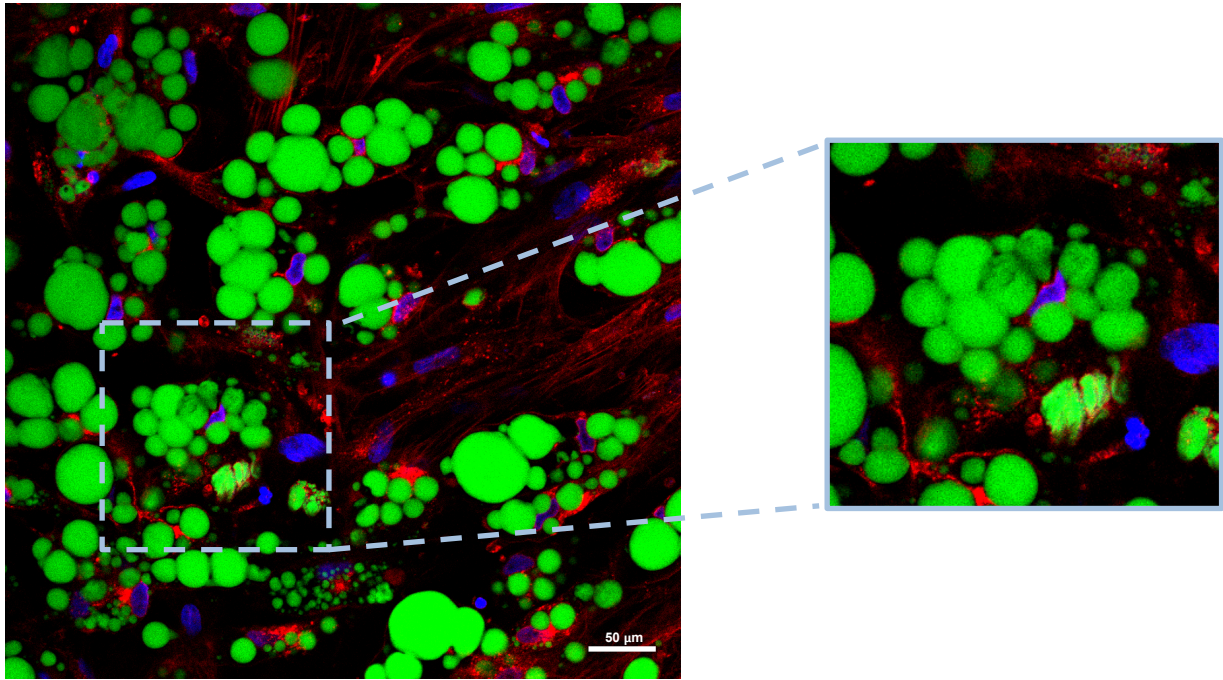
(C) Line charts displaying gene expression trends (normalized mRNA expression values; $\Delta\Delta Ct = \Delta Ct \text{ sample} - \Delta Ct \text{ reference sample}$) measured by qPCR. PPIA was used as reference gene for all analyzed genes. For each gene, the first time point showing detectable mRNA levels was used as reference ($\Delta\Delta Ct = 0$). Data are reported as mean from three independent experiments.

(D) Line charts showing gene expression variations between two subsequent time points ($\Delta\Delta Ct \text{ time point 2} - \Delta\Delta Ct \text{ time point 1}$) along hMSCs differentiation determined by qPCR. PPIA was used as reference gene and data are reported as mean from three independent experiments.

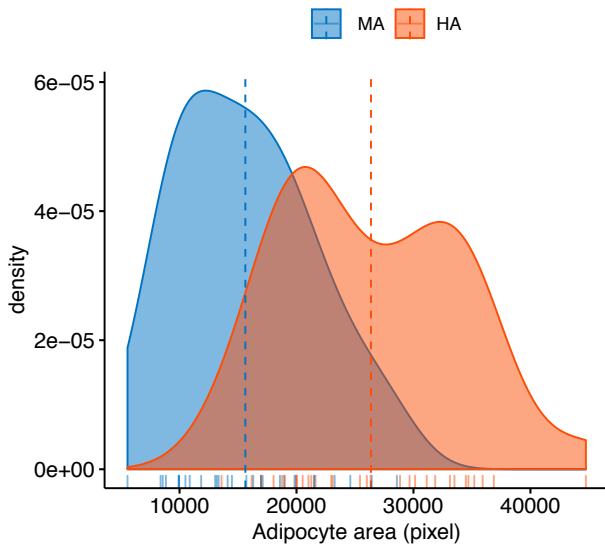
(E) Line charts comparing gene expression trends - analyzed as in panel C - of cPPARG and MRTFA genes along hMSCs differentiation. Similar expression trends at specific time points are indicated by light green boxes (from T=0 hours to T=6 days, from MA to HA) and opposite trends in stages indicated by yellow box (from T=6 days to MA).

Figure S6

A



B



C

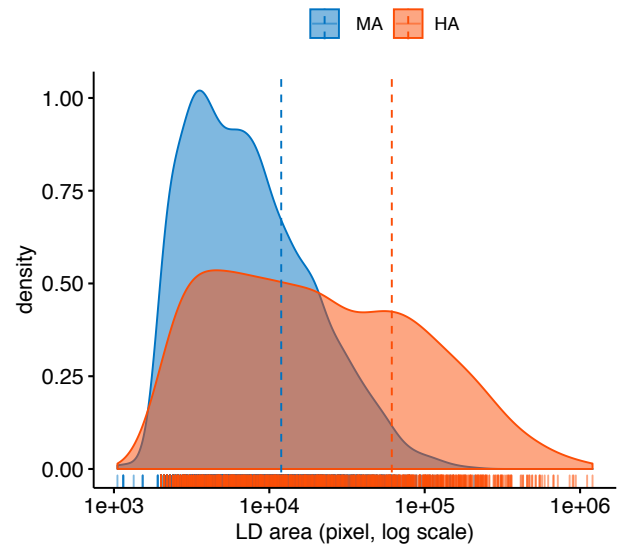


Figure S6. Morphometric characteristics of hypertrophic-like adipocytes

(A) Representative confocal microscopy images displaying a marked *nuclei* pressure in hypertrophic-like adipocytes stained with DAPI (*nuclei*, blue), Bodipy 495/503 (lipid droplets, green) and WGA 632/647 (cell membranes, red; scale bar, 50 μ m).

(B-C) Density plots showing value distribution of (B) adipocyte area - analyzed on MAs (n=30) and HAs (n=30) - and (C) lipid droplets area measured on 2973 LDs (from 214 MAs) and on 1168 LDs (from 206 HAs).

Figure S7

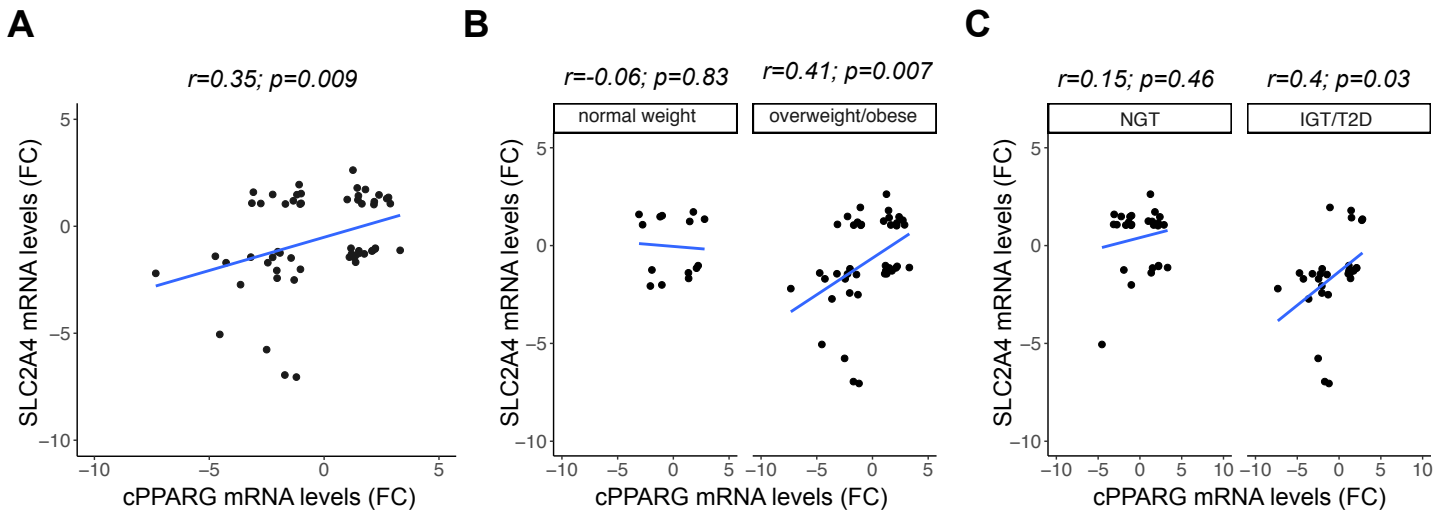


Figure S7. The expression of canonical *PPARG* transcripts correlates with *SLC2A4* levels

cPPARG expression was previously measured in Aprile et al., 2018.

(A-C) Scatterplot reporting the correlation by linear regression analysis between *SLC2A4* and cPPARG expression levels (qPCR) in the SAT of a subset of individuals (N=56); stratified in subgroups according to BMI in normal weight (N=14) and overweight/obese (N=42), or to glucose-metabolizing capacity in NGT (N=27), IGT and T2D (N=29). *RPS23* was used as reference gene. Pearson's correlation coefficient (r) and p values (p) are shown.

Table S1. Sequences of oligonucleotides used in RT-PCR and qPCR assays

Gene	Sense Primer (5'-3')	Antisense Primer (5'-3')	Melting Temperature (°C)	PCR product (bp)	Reference figure
<i>cPPARG</i>	GAGAAGGAGAAGCTGTTGCC	ATGGCCACCTCTTTGCTCT	60	272	1B-C-D; 3C; 4A-B; 6F-G; 7A-B-C; S5B-C-D-E; S7A-B-C
<i>ADIPOQ</i>	CTGGTGAGAAGGGTGAGAAA	GTTCTCCTTTCCTGCCTTGG	60	126	3C; 4A-B; 6G; S5B-C-D
<i>FABP4</i>	TGTGTGATGCTTTTGTAGGTAC	CTTCGTCAAATTCCTGGCCC	60	215	3C; 4A-B; 6G; S5B-C-D
<i>LPL</i>	CGCCGCCGACCAAAGAAGA	AGGTAGCCACGGACTCTGC	60	122	4A-B; 6G
<i>PPARGΔ5</i>	CTTGCACTGGGGATGTCTCA	CAGCAAACCTGGGCGGTGA	60	242	1A-C-D; 6F-G; S5A
<i>PPIA</i>	TACGGGTCCTGGCATCTTGT	GGTGATCTTCTTGCTGGTCT	60	196	3C; 4A-B; 6F-G; S5A-B-C-D-E
<i>MRTFA</i>	TTGAAACTCCAGCAGCGCC	GCTCCTTCTCTGCTCATGA	60	99	4A-B; 6G; S5B-E
<i>SLC2A4</i>	CGTCGGGCTTCCAACAGAT	GAGCCAAGCACCGCAGAGA	60	100	3C; 4A-B; 6G; 7A-B-C; S5B-C-D; S7A-B-C
<i>PLIN1</i>	GCCTCACCTTGCTGGATGG	GTGGGCTTCCTTAGTGCTG	60	128	3C; 4A-B; 6G; S5B-C-D
<i>PLIN2</i>	GGGCTAGACAGGATTGAGGA	TCACTGCCCTTTGGTCTTG	60	181	3C; 4A-B; 6G; S5B-C-D
<i>IRS2</i>	TACATCGCCATCGACGTGAG	TCAATGCTGGCGTAGGTGTT	60	215	3C; 4A-B; 6G
<i>RPS23</i>	TCGTGGACTTCGTA CTGCT	GCTGTGATTTTCTTGCCATTC	60	237	1A-B-C-D; 7A-B-C; S7A-B-C
<i>PPARG1</i>	CGAGGACACCGGAGAGGG	TGTGTCAACCATGGTCATTTTC	60	135	S5A
<i>PPARG2</i>	TCCATGCTGTTATGGGTGAA	TGTGTCAACCATGGTCATTTTC	60	113	S5A

Table S2. Reagents and resources information

REAGENT	SOURCE	IDENTIFIER
Antibodies		
PPAR γ (C26H12) Rabbit mAb (N terminus)	Cell Signaling Technology	Cat# 2435
GLUT-4 Polyclonal Antibody	Elabscience	Cat#E-AB-30268
ADIPOQ Polyclonal Antibody	Elabscience	Cat#E-AB-40301
FABP4 Polyclonal Antibody	Elabscience	Cat#E-AB-60028
IRS2 Polyclonal Antibody	Elabscience	Cat#E-AB-62281
HSP90AA1 Mouse Monoclonal Antibody	Origene	Cat# TA500883
Goat Anti-Mouse IgG (H L)-HRP Conjugate	Bio-Rad	Cat# 170-6516
Goat Anti-Rabbit IgG (H L)-HRP Conjugate	Bio-Rad	Cat# 170-6515
Biological Samples		
Subcutaneous adipose tissue cDNA samples of a Geman cohort of patients	Prof. Matthias Blüher. (Keller et al., 2016; Guiu-Jurado et al., 2016)	N/A
Chemicals, Peptides, and Recombinant Proteins		
DMEM/F-12, no glutamine	Thermo Fisher Scientific	Cat# 21331020
Fetal Bovine Serum Origin: EU Approved (South American)	Thermo Fisher Scientific	Cat# 10270106
Fetal Bovine Serum, qualified, Australia	Thermo Fisher Scientific	Cat# 10099141
Penicillin-Streptomycin (5,000 U/mL)	Thermo Fisher Scientific	Cat# 15070063
L-Glutamine (200 mM)	Thermo Fisher Scientific	Cat# 25030081
BMP4 Recombinant Human Protein	Thermo Fisher Scientific	Cat# PHC9534
Troglitazone	Sigma Aldrich	Cat# T2573
Rosiglitazone	Sigma Aldrich	Cat# R2408
Cycloheximide	Sigma Aldrich	Cat# 01810
GW9662	Sigma Aldrich	Cat# M6191
Insulin (Humulin R)	Lilly	Cat# AIC025707011/M
Dexamethasone	Sigma Aldrich	Cat# D4902
Isobutyl-1-methylXanthine	Sigma Aldrich	Cat# I7018
Biotin	Sigma Aldrich	Cat# B4639
D- Pantothenic acid hemicalcium	Sigma Aldrich	Cat# P5155
Pierce IP Lysis buffer	Thermo Fisher Scientific	Cat# 87787
Halt Protease	Thermo Fisher Scientific	Cat# 78429
Phosphatase Inhibitor Cocktail	Thermo Fisher Scientific	Cat# 78420
Oil red O staining	Sigma Aldrich	Cat# O1391
Bodipy 493/503	Thermo Fisher Scientific	Cat# D3922
DAPI (4',6-Diamidino-2-Phenylindole, Dihydrochloride)	Thermo Fisher Scientific	Cat# D1306
Wheat Germ Agglutinin, Alexa Fluor™ 633 Conjugate	Thermo Fisher Scientific	Cat# W21404
Quick Start™ Bradford 1x Dye Reagent	Bio- Rad	Cat# 5000205
Pierce™ ECL Western Blotting Substrate	Thermo Fisher Scientific	Cat# 32209
Commercial Assays		
High Capacity cDNA Reverse Transcription kit	Thermo Fisher Scientific	Cat# 4368814
Experimental Models: Cell Lines		
hTERT immortalized Adipose Derived Mesenchymal Stem Cells	ATCC	Cat# SCRC4000
Software and Algorithms		
R Bioconductor package	Tarazona et al., 2011	https://www.bioconductor.org/
FACSDiva software		https://www.bdbiosciences.com
GelQuant.NET software		https://www.biochemlabsolutions.com
ImageJ	Abramoff et al., 2004	https://imagej.net/Citing